Report

Current Biology

Chemokine-Dependent pH Elevation at the Cell Front Sustains Polarity in Directionally Migrating Zebrafish Germ Cells

Graphical Abstract

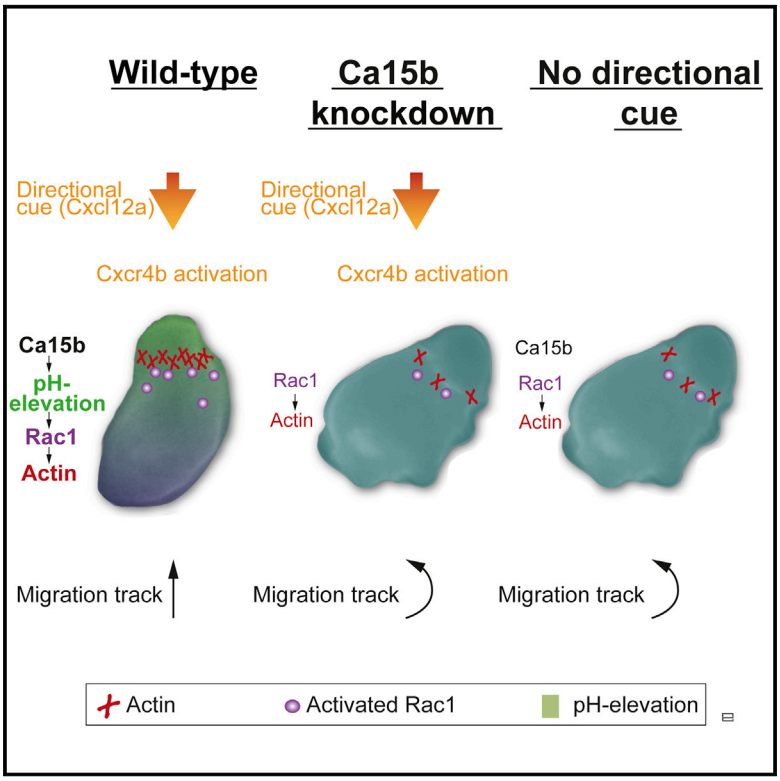

Highlights

- Migrating PGCs elevate pH at the cell front in response to chemokine signaling
- Elevated pH at the cell front maintains cell polarity in vivo
- The elevated pH increases Rac1 activity and actin polymerization at the cell front

Authors

Katsiaryna Tarbashevich, Michal Reichman-Fried, Cecilia Grimaldi, Erez Raz

Correspondence

erez.raz@uni-muenster.de

In Brief

Tarbashevich et al. reveal a mechanism for cell polarization in vivo in response to chemokine signaling, where the cell responds to the graded distribution of the guidance cue by establishing elevated pH at the cell front. The elevation in the pH promotes Rac1 activity and actin polymerization at the leading edge of the migrating cells.

Tarbashevich et al., 2015, Current Biology *25*, 1096–1103
April 20, 2015
http://dx.doi.org/10.1016/j.cub.2015.02.071

CellPress

Current Biology
Report

Chemokine-Dependent pH Elevation at the Cell Front Sustains Polarity in Directionally Migrating Zebrafish Germ Cells

Katsiaryna Tarbashevich,[1] Michal Reichman-Fried,[1] Cecilia Grimaldi,[1] and Erez Raz[1,*]
[1]Institute for Cell Biology, Center for Molecular Biology of Inflammation, Münster University, Von-Esmarch-Strasse 56, 48149 Münster, Germany
*Correspondence: erez.raz@uni-muenster.de
http://dx.doi.org/10.1016/j.cub.2015.02.071

SUMMARY

Directional cell migration requires cell polarization with respect to the distribution of the guidance cue. Cell polarization often includes asymmetric distribution of response components as well as elements of the motility machinery. Importantly, the function and regulation of most of these molecules are known to be pH dependent [1–3]. Intracellular pH gradients were shown to occur in certain cells migrating in vitro [4–6], but the functional relevance of such gradients for cell migration and for the response to directional cues, particularly in the intact organism, is currently unknown. In this study, we find that primordial germ cells migrating in the context of the developing embryo respond to the graded distribution of the chemokine Cxcl12 by establishing elevated intracellular pH at the cell front. We provide insight into the mechanisms by which a polar pH distribution contributes to efficient cell migration. Specifically, we show that Carbonic Anhydrase 15b, an enzyme controlling the pH in many cell types [7–9], including metastatic cancer cells [6], is expressed in migrating germ cells and is crucial for establishing and maintaining an asymmetric pH distribution within them. Reducing the level of the protein and thereby erasing the pH elevation at the cell front resulted in abnormal cell migration and impaired arrival at the target. The basis for the disrupted migration is found in the stringent requirement for pH conditions in the cell for regulating contractility, for the polarization of Rac1 activity, and hence for the formation of actin-rich structures at the leading edge of the migrating cells.

RESULTS AND DISCUSSION

Establishment and maintenance of distinct pH values in different cellular domains are crucial for normal cell and organ function (reviewed in [10]). Abnormal pH regulation, for example, can detrimentally affect heart and kidney function by leading to osteopetrosis and lysosomal storage disease [11] (reviewed in [10]). Cellular pH is also an important variable in the context of cell migration where it has been suggested to play a role in the regulation of neutrophils chemotaxis [12], wound healing (reviewed in [5]), and tumor cell metastasis (reviewed in [3]). Specifically, different motile cell types, including cancer cells, exhibit pH gradients such that the intracellular pH is elevated at the front of a migrating cell relative to its back [4]. In the case of cancer-cell dissemination, the pH is thought to play a role in regulating cell adhesion, cytoskeletal dynamics, and the reorganization of the extracellular matrix [3]. To examine the mechanisms of pH control in migrating cells and the role it plays in an in vivo setting, we set out to investigate these issues in zebrafish primordial germ cells (PGCs) because these cells share several properties with metastatic cancer cells, including motility initiation, mode of migration, and response to chemotactic cues [13–18].

To visualize pH distribution in PGCs, we made use of the fluorescence resonance energy transfer (FRET)-based intramolecular ratiometric pH biosensors Cy11.5 (pHlameleon 5) [19] and pHlameleon 6, along with the pHlameleon 7 version that does not FRET under physiological conditions in PGCs, thus serving as a negative control [20] (Figures S1A–S1D; Movie S1). Global expression of biosensors revealed similar pH index ratios for somatic cells and PGCs as measured at 6 hours post fertilization (hpf) using both pH reporters (Figures S1B–S1D). pHlameleon 5 provided higher FRET values than pHlameleon 6 (Figures S1B–S1D), in agreement with results previously obtained in Chinese hamster ovary (CHO) cells [20]. Based on these preliminary experiments, we chose to use pHlameleon 5 and targeted protein expression preferentially to PGCs by fusing its open reading frame (ORF) to the *nanos1* 3′ UTR ([21]. We found that during "run" phases, when PGCs are morphologically polar and actively migrate [22], the cells exhibit a polarized pH distribution, where the pH is elevated at the cell front (see Figure S1E for measurement strategy), similar to that generated in disseminating cancer cells (Figure 1A, left [4, 6, 20]). In contrast, during tumbling phases, when PGCs lose polarity and pause [22], uniform pH distribution was observed, with local pH elevation in the forming blebs (Figure 1A, right). As a control for these measurements, we made use of the CFP protein, which did not exhibit a differentially distributed FRET signal within the cells (Figure S1F). Whereas using two other protein reporters to determine the pH distribution in the cell confirmed our results ([23, 24], sfGFP and its optimized version sfGFP^{T203C} both

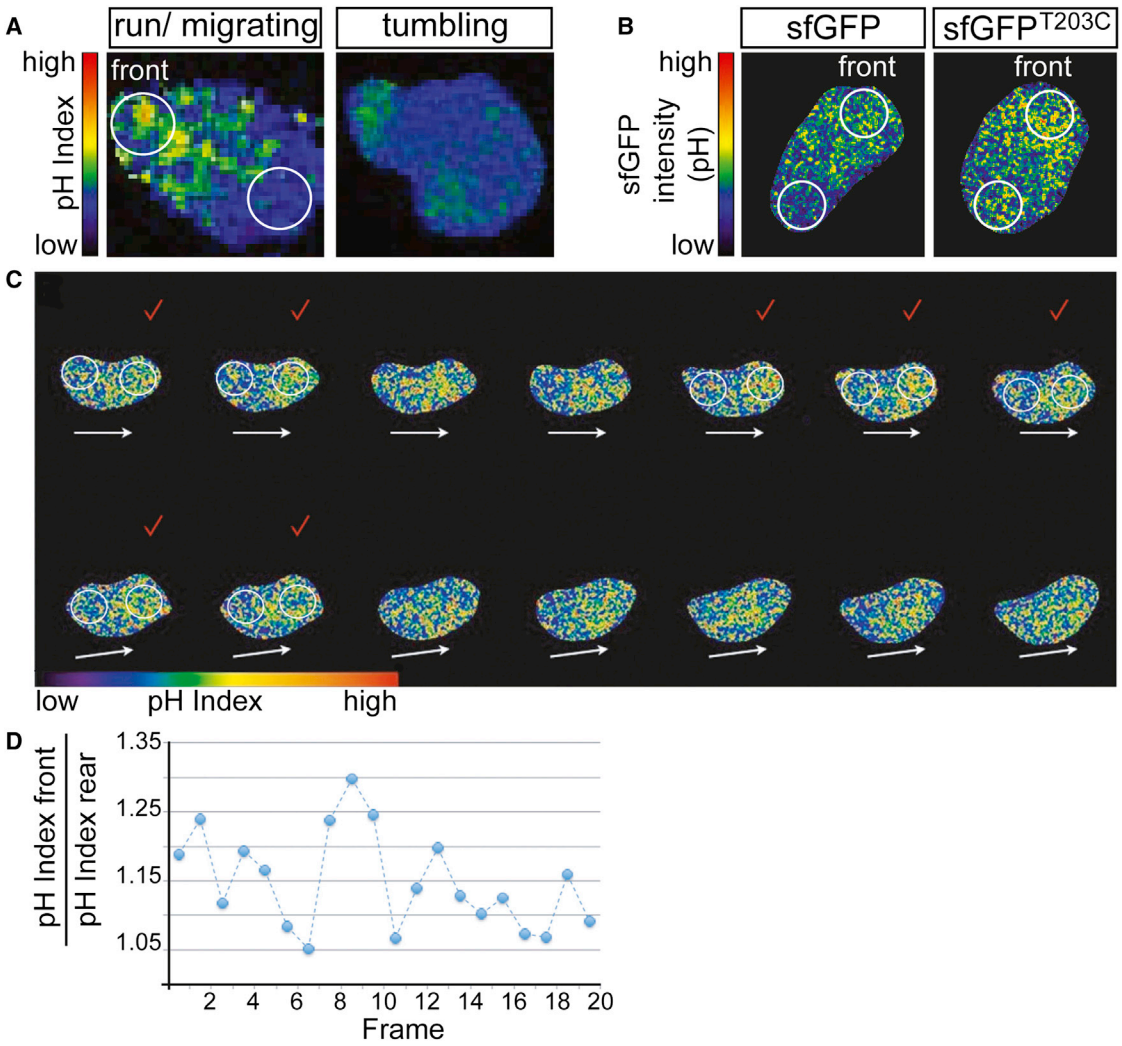

Figure 1. pH Is Elevated at the Front of Migrating PGCs

(A) Representative images of pH distribution in migrating (polar) and tumbling (apolar) PGCs using the pHlameleon 5 pH sensor. Images of PGCs were acquired at 6 hpf using an epifluorescence microscope.

(B) Images of representative PGCs expressing super folder (sf)GFP-mCherry and sfGFP^{T203C}-mCherry tandem proteins. pH scale corresponds to sfGFP fluorescence intensity normalized to that of mCherry fused to it.

(C) Snapshots from a time-lapse movie of a representative migrating PGC, presenting pH elevation at the cell front. The movie was acquired at 7.5-s intervals, and time points (T0 upper left) in which pH elevation is observed are labeled with a red check mark.

(D) Graph showing front/rear pHlameleon 5 pH index ratios for 20 sequential frames from a time-lapse movie acquired using a confocal microscope. Measurements are derived from the areas circled in white at the front and rear of cells included in and extended from (C). Arrows in (C) indicate the direction of migration.

normalized to mCherry; Figures 1B and S1G), we chose to use the pHlameleon 5 reporter in subsequent experiments because of the enhanced photostability and broader dynamic range it offers. Taken together, the pH profile in migrating PGCs appears to be reminiscent of that observed in tumor and immune cells in vitro [4, 6, 12].

We subsequently examined PGCs with the aim to determine the dynamics and the regulation of the pH at a high temporal and spatial resolution in an in vivo context. Unlike the stable pH profile described for cells migrating in culture (e.g., pH 8), applying high temporal resolution in vivo revealed that the pH distribution within the PGCs is dynamic. Namely, during the run phases, a clear pH elevation at the cell front was observed in 30%, on average, of the movie frames (Figure 1C; Movie S2, left cell). Comparison of the pH index levels between the front and rear of the cells during run phases revealed a relative elevation of up to 30% at the front, with an average elevation of 7% (Figure 1D; FRET analysis is described in Supplemental Experimental Procedures). This difference in pH index corresponds to 0.2 pH units (calculated based on calibration experiments performed using the Nigericin ionophore, as explained in Supplemental Experimental Procedures). The frequency as well as the duration of higher pH periods at the cell front appeared to fluctuate (Figures 1C and 1D).

To explore the mechanisms responsible for establishing the polar pH distribution, we searched for proteins that could potentially control this process. Our interest was focused on the carbonic anhydrases group of enzymes [3] that catalyze the reversible inter-conversion of carbon dioxide and water to bicarbonate and protons and thus regulate cellular pH [9, 25]. The corresponding carbonic anhydrase genes were shown to be expressed in zebrafish PGCs [26] and particularly *carbonic anhydrase 15b* (*ca15b*), whose RNA was found to be 15-fold enriched in these cells at the time of migration onset relative to somatic cells [26]). Further analysis of the gene expression proved that *ca15b* was the only *carbonic anhydrase* gene that exhibited enrichment in PGCs during their migratory phase, and its expression was more pronounced than that of the *nanos3* RNA encoding for the universal PGC-expressed RNA-binding protein Nanos [21, 27–29] (Figure S2 demonstrates this point qualitatively). *ca15b* mRNA is a maternally provided transcript expressed in the blastomeres and in the germplasm during early cleavage stages (Figure 2A). At the time PGCs normally migrate toward the region where the gonad develops (4–24 hpf), *ca15b* mRNA is expressed exclusively in germ cells. A similar expression pattern of the *ca15b* RNA was recently described by Wang et al. [30].

To determine the role Ca15b may play in migration and in controlling pH dynamics in PGCs, two translational blocking morpholino oligonucleotides were employed that specifically target the gene. We first measured the total (i.e., from the whole cell) pH index values in control PGCs and in the Ca15b knockdown counterparts and observed a significant decrease in the average pH index values in *ca15b* morphants, reflecting a reduction in the pH (Figures 2B, bottom, and 2C, PGCs). This effect was reversed upon introduction of morpholino-insensitive *ca15b* transcripts (Figures 2B, bottom, and 2C, PGCs). It is noteworthy that somatic cells in this experiment did not show any changes in pH index values, thus providing an additional confirmation for the specificity of the method (Figure 2C, somatic cells). Significantly, germ cells knocked down for Ca15b function, in addition to showing a global reduction in pH, no longer exhibited the pH elevation at the front (determined as an average of 20 time-lapse movie frames; Figures 2B and S1E; Movie S2, right cell). In this experiment, too, the specific targeting of *ca15b* transcripts by two different morpholinos was verified as the knockdown effect was eliminated when *ca15b* RNA rendered insensitive to the antisense-oligonucleotide was provided to the treated cells (Figure 2B, bottom). Since *morpholino 2* (*MO2*) appeared to be more effective than *MO1*, *MO2* was used in most of the experiments described hereafter.

It is interesting to note that Ca15b protein appears to represent a unique member in the Ca15 subgroup of carbonic anhydrases, since it lacks a secretion peptide sequence and thus acts within the cells that express it. Other Ca15 proteins were reported to face the extracellular space, where they carry out their function [9, 31].

To determine whether Ca15b function is required for normal migration of the germ cells, we followed the process in embryos in which the translation of the protein was inhibited. We found that 20% of the PGCs in *ca15b* morphants failed to reach their migration target, reflecting a 2-fold increase in the number of ectopic cells relative to control embryos. This phenotype was reverted to that of wild-type in the presence of MO-insensitive *ca15b* mRNA (Figure 3A). Thus, directionally migrating PGCs lacking the pH elevation at the front were more likely to reach ectopic locations. We tested the idea that the manipulated cells might be defective in their response to the attractive cue in the environment. Consistent with this notion, we found that reducing the level of the Cxcl12a, the chemokine that constitutes the guidance cue to migrating PGCs, further increased the effect of Ca15b knockdown. Specifically, targeting *ca15b* translation in embryos heterozygous for a mutation in the *cxcl12a* gene enhanced the morpholino-induced phenotype such that here, 40% of the PGCs were found at ectopic positions in 24 hpf embryos (Figure 3B). This finding is in agreement with the idea that PGCs response to Cxcl12a is mediated, at least in part, by controlled distribution of pH in the cell. We were therefore prompted to examine the possibility that Cxcl12a plays a role in controlling the pH distribution in the migrating cells. Toward this end, we initially eliminated the chemokine gradient by either knocking down Cxcl12a or by expressing it uniformly throughout the embryos. We also interfered with the ability of the cells to respond to Cxcl12 cues by inhibiting the translation of the chemokine receptor Cxcr4b, or by inhibiting the Gα-dependent signaling cascade downstream to the chemokine receptor through expression of pertussis toxin (Ptx) in PGCs [32, 33]. Strikingly, all these experiments resulted in elimination of the polar pH distribution in PGCs (Figure 2B). In addition, we assessed the global pH in the cells after knockdown of Cxcr4b, overexpression of Cxcl12a, and overexpression of Ca15b. These experiments revealed a mild increase in pH in the cases of Cxcl12a and Ca15b overexpression and a reduction in the pH when Cxcr4b was knocked down (Figure 2D). We thus conclude that the main function of chemokine signaling in this context is to initiate a cascade leading to polarized pH distribution that depends on Ca15b function, rather than to regulate the global pH in the cells.

Together, pH elevation at the front of migrating PGCs relies on Ca15b function and on the ability of the germ cells to respond to the chemoattractant signal. While PGCs are able to polarize in the absence of Cxcl12a-enconded directional cues, the polarity is reduced and the migration of the cells is characterized by shorter run phases [22, 32]. Our findings suggest therefore that the polar pH distribution constitutes one of the cellular responses to the polarized chemokine signal and that this response contributes to maintaining cell polarity downstream of Cxcl12a.

To determine the precise role of pH elevation at the cell front in PGC migration, we analyzed individual migration tracks of PGCs. Intriguingly, the migration tracks of *ca15b* morphant PGCs exhibited reduced straightness, a parameter that indicates how many turns are made by a cell while migrating. Accordingly, reduced straightness signifies more changes in migration direction and thus a reduced polarity (Figures 4A and S3A). To further address the effect of Ca15b knockdown in a different and a simplified experimental setup, we analyzed the migration of PGCs toward a Cxcl12a source that was artificially positioned in the embryo (Figure S3B). We found that similar to the previous experiment, migrating PGCs from *ca15b* morphants formed migration tracks that showed reduced straightness as well as reduced displacement (Figures S3C–S3E; Movie S3).

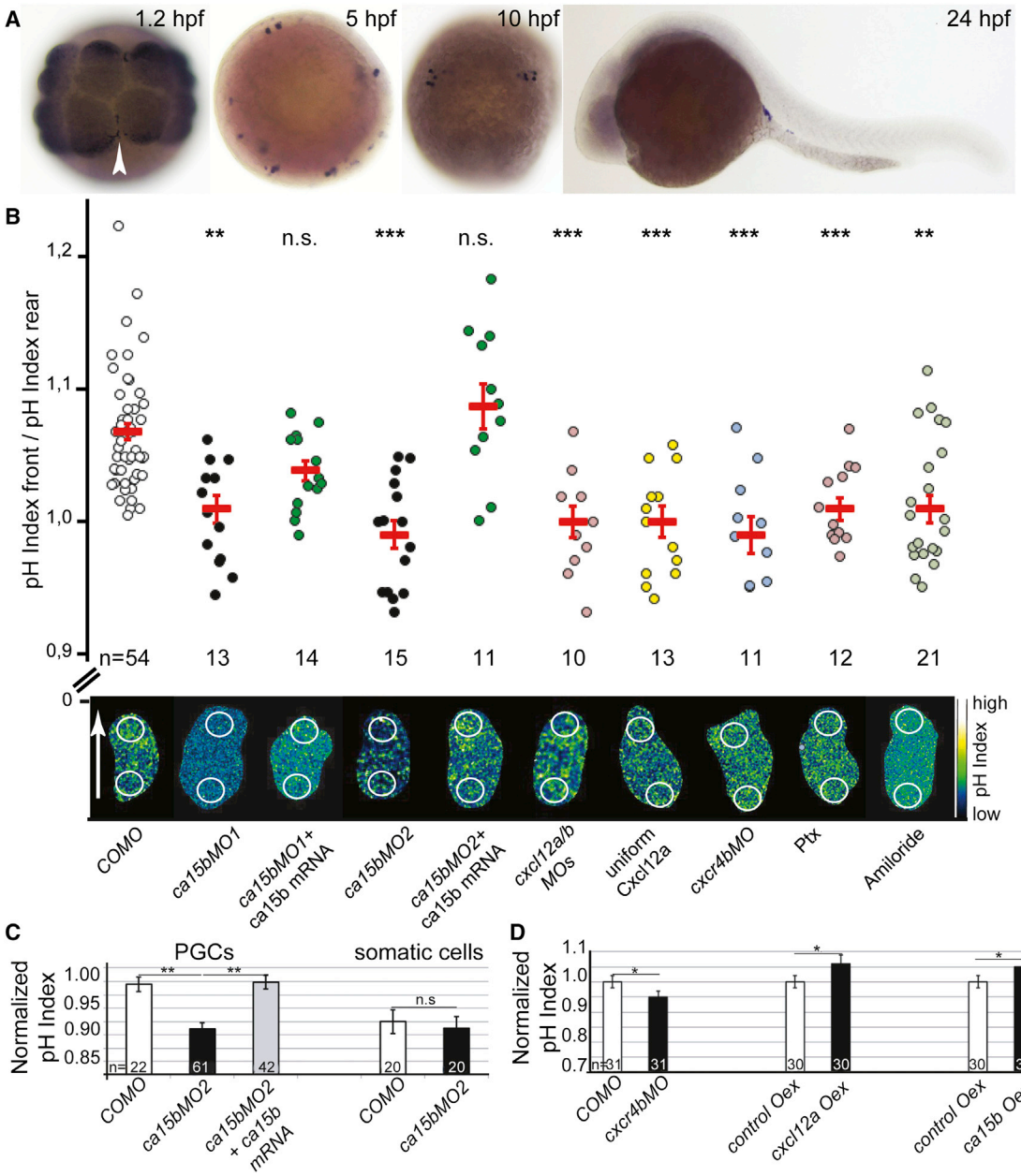

Figure 2. Ca15b and Cxcl12 Signaling Control the Polar pH Distribution in PGCs

(A) Expression pattern of *ca15b* RNA in embryos at 1.2, 5, 10, and 24 hpf (blue staining). The arrowhead points at the position of the germplasm.

(B) Polar pH distribution in PGCs depends on the function of Ca15b, on Cxcl12 chemokine gradient, on G protein signaling, and on Na^+/H^+ exchangers. The graph presents average pH index ratios between the front and the rear of migrating PGCs in 7–8 hpf embryos injected with the following: control morpholino (*COMO*), *ca15b* morpholino (*ca15bMO1* and *ca15bMO2*), *ca15b* morpholino 1 and 2 along with morpholino-insensitive *ca15b* mRNA to restore Ca15b function, combined Cxcl12a and Cxcl12b morpholinos (*cxcl12a/b MOs*) for chemokine depletion, *cxcl12a* RNA for uniform Cxcl12a distribution, *cxcr4b* morpholino (*cxcr4bMO*), and *Ptx* RNA for disruption of the chemokine signaling pathway. Embryos were soaked in amiloride to interfere with the activity of Na^+/H^+ exchangers. Lower panel of images presents examples of PGCs with the corresponding treatments. Images were acquired using a confocal microscope. White circles depict areas at the front and back of PGCs used for pH index measurements. The white arrow indicates the direction of migration.

(C) Graphs show average whole-cell pH index intensity values in PGCs and somatic cells at 6–7 hpf following knockdown and restoration of Ca15b activity (labeling as in B).

(D) Graph presenting average global pH index levels in PGCs subjected to *cxcr4b* knockdown (*cxcr4bMO*) and Cxcl12a or Ca15b overexpression (Oex). n denotes the number of PGCs analyzed. *p < 0.05, **p < 0.01, ***p < 0.001 as determined by the Student's t test. Error bars represent SEM.

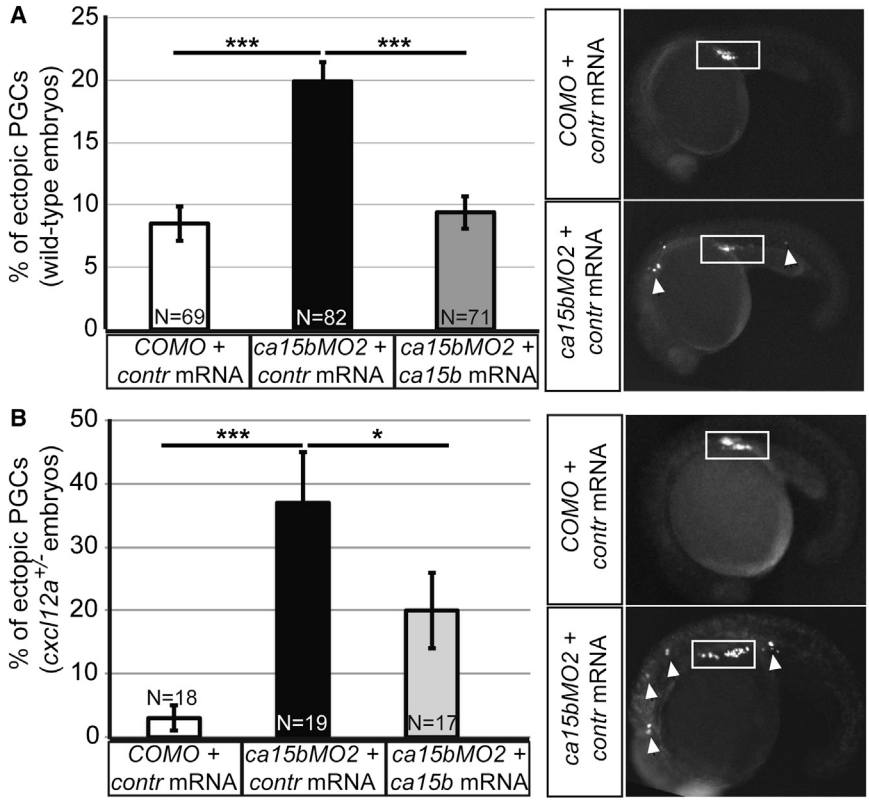

Figure 3. *ca15b* Knockdown Impairs PGC Migration

(A) Graph shows the percentage of ectopic PGCs from total PGC number in wild-type embryos at 24 hpf.

(B) Graph presents the average percentage of ectopic PGCs in 24 hpf embryos heterozygous for a mutation in *cxcl12* (*medusa* mutation). Right panels show representative images of the PGC positioning in control and *ca15b* morphant embryos in wild-type (A) and in *medusa*$^{+/-}$ embryos (B).

N is number of embryos analyzed. White boxes depict the normal position of PGCs in 24 hpf embryos, arrowheads point at PGCs located in ectopic positions. *p < 0.05, ***p < 0.001 as determined by the Student's t test. Error bars depict SEM.

To establish the basis for the defective migration of cells with decreased Ca15b activity, we compared the behavior and shape of manipulated cells with those of control cells. It became apparent that the total amount of blebs is significantly elevated in PGCs upon Ca15b knockdown (Figure 4B). This phenotype was reversed by providing the cells with MO-resistant *ca15b* RNA (Figure 4B). In addition, unlike control cells that extended blebs primarily at the cell front, PGCs knocked down for Ca15b formed blebs at the cell rear at a high frequency (observed in 10 of 40 cells) (Figures 4C and S4A; Movie S4).

Since myosin activity is involved in bleb formation [34] and because at a lower pH, Ca^{2+}- and pH-dependent calmodulin undergoes conformational changes and consequently induces MLCK (myosin light-chain kinase) activation (reviewed in [3, 35]), we reasoned that phosphorylation of myosin light chain (MLC) could be affected in *ca15b* morphant PGCs with lower pH. We therefore examined the phosphorylation of MLC (pMLC) as a measure for myosin activity [36, 37] and compared between control and *ca15b* morphant PGCs. Consistent with this rationale, we could observe an elevated level of pMLC in *ca15b* morphant PGCs, which reverted to the control levels by the introduction of the MO-resistant *ca15b* RNA (Figure 4D; controls for this experiment are presented in Figures S4B and S4C). Thus, higher levels of pMLC would explain the increased blebbing in cells with reduced Ca15b activity.

Considering the defective PGC migration in *ca15b* morphant embryos as judged by the altered migration tracks and inefficient arrival at the target, we next examined whether other aspects of cell motility were influenced by the polar pH distribution in motile PGCs. To this end, we focused on Rac1, a member of the Rho-GTPase family and a key regulator of actin dynamics. Pertinent to this context is the fact that Rac1 requires a higher pH for its optimal activity in promoting actin polymerization ([1, 38]. Intriguingly, at the front of migrating germ cells, the elevated pH as described here appears to align with an elevated activity of Rac1 as previously described [39]. Indeed, a significant decrease in Rac1 activity was observed in cells knocked down for the Ca15b protein that lack the polar pH distribution (Figure 4E) along with reduced actin polymerization at the front of these cells (Figure 4F).

In addition to the controlling actin polymerization by regulating Rac1 activity, the distribution of the pH within the cell could also affect the function of actin-severing proteins such as ADF or cofilin whose activity was shown to be dependent on pH conditions [40]. To determine whether enhanced blebbing in a PGC can modulate global pH, we expressed constitutively active MLCK in PGCs and found no significant change in pH index levels (Figure S4D). Furthermore, we did not observe any effect of pH reduction on the activity of another GTPase, RhoA (Figure S4E; control measurements for the RhoA activity are presented in Figure S4F). These findings are consistent with the idea that pH conditions in the cell determine the level of contractility while contractility per se has no effect on the pH.

In conclusion, in this report we describe for the first time an elevation of pH at the front of migrating PGCs in the context of the live organism. We show that the polarized pH distribution depends on a polarized chemokine signal and on the function of Carbonic Anhydrase 15b. The precise molecular cascade linking Cxcl12a/Cxcr4b signaling and Ca15b function to the observed elevation in the pH is unknown. One could consider, however, the possible involvement of regulation of ion channel activity by Ca^{2+} influx, where the latter normally occurs downstream

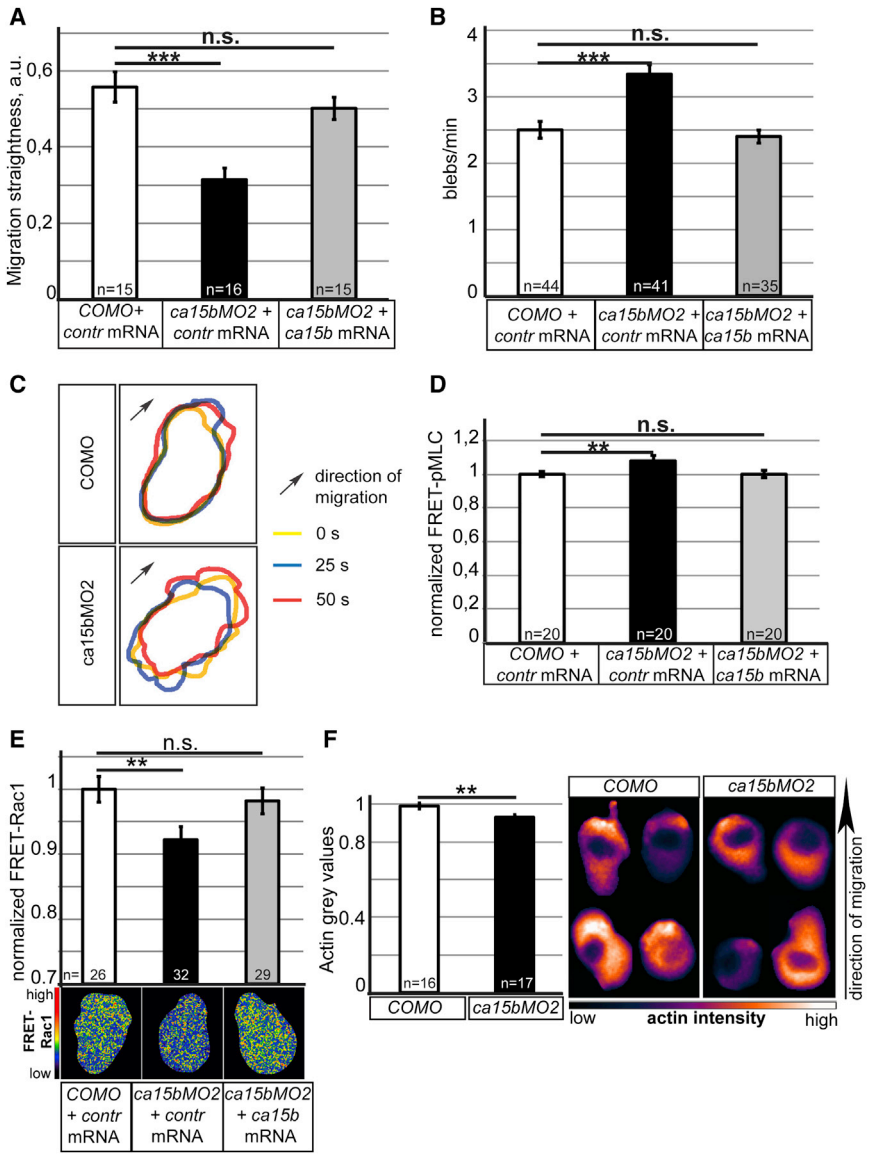

Figure 4. Ca15b Activity Modulates PGC Behavior, Actin Polymerization, and Contractility

(A) Graph shows the average straightness of tracks formed by migrating PGCs in control embryos versus those in embryos knocked down for Ca15b. The individual tracks are presented in Figure S3A.

(B) Graph represents the average frequency of bleb formation in control embryos versus in embryos knocked down for Ca15b.

(C) Panels illustrate overlays of contours of a migrating PGC at 0, 25, and 50 s of image acquisition. Analysis was performed for a control PGC (top) and a *ca15b* morphant PGC (bottom).

(D–F) Ca15b sustains polarized protrusive activity, graded Rac1 activity, and elevated actin polymerization at the cell front. (D) MLC phosphorylation, indicating myosin activity, is presented in the graph as average FRET-pMLC ratios in PGCs of embryos knocked down for Ca15b relative to controls at 7–8 hpf. (E) Levels of Rac1 activity are presented in the graph as average Rac1-FRET ratios in PGCs following knockdown of Ca15b. Representative images of Rac1-FRET ratios in control (*COMO*) and *ca15b* morphant (*ca15bMO2*) PGCs as well as in *ca15b* morphant cells with restored Ca15b activity are below the graph. (F) Actin levels are presented in the graph as average intensities of actin labeling in embryos knocked down for Ca15b (*ca15bMO2*) relative to controls (*COMO*) (for the detailed analysis protocol, see Supplemental Experimental Procedures). Presented in the right panels are representative examples of actin in migrating control and *ca15b* morphant PGCs.

FRET-pMLC and FRET-Rac1 ratios were normalized relative to the corresponding average control values. n denotes the number of PGCs analyzed. $^{**}p < 0.01$, $^{***}p < 0.001$ as determined by the Student's t test. Error bars depict SEM.

to chemokine receptor activation. For example, the interaction between Na^+/H^+ exchanger isoform 1 (NHE1) and Ca-calmodulin, as previously demonstrated (reviewed in [41, 42]), could cooperate with Ca15b. In line with this possibility is the finding that inhibition of the NHE activity by the application of amiloride severely affects pH elevation at the front of migrating germ cells (Figure 2B). The resultant pH distribution pattern appears to be critical for polarizing the protrusive activity of the cells to the front as well as for elevating actin polymerization at this part of the cell. We suggest that this cellular asymmetry is critical for the polarization of the cell relative to the guidance cue and contributes to an effective directed migration toward the sources of the chemoattractant. Importantly, similar mechanisms of cellular polarization may be relevant for disseminating metastatic cells. In this case, the low extracellular pH in front of the migrating cancer cell was shown to activate matrix metalloproteinases (MMPs) and assist extracellular matrix (ECM) dissociation ([6, 41]). While the functional significance of the finding was not investigated, an elevation in pH at the cell front was described for a melanoma cell line in vitro [4]. As we show here, such a distribution of pH in metastatic cells could potentially facilitate Rac1 activity and actin polymerization, thereby stimulating the formation of invadopodia in the direction of invasion. Further investigations aimed at deciphering the functional significance of intracellular pH conditions for cell migration and studies aimed at understanding the mechanisms regulating the intracellular pH distribution in cell motility and guided migration are thus highly relevant for understanding the process of metastasis and the design of cancer therapies.

EXPERIMENTAL PROCEDURES

Experimental design, amounts of injected mRNAs, and MOs are listed in Supplemental Experimental Procedures. The zebrafish were handled according to the law of the state of North Rhine-Westphalia, supervised by the veterinarian office of the city Münster.

Epifluorescence Microscopy

Epifluorescence microscopy was performed using an AxioImager.M1 microscope (Zeiss) with an RTSlider camera (Visitron) controlled by VisiView software (Visitron).

Low-magnification (10–20×) time lapses were acquired at 6–8 hpf every 2 min. Data analysis was performed using MetaMorph (Molecular Devices) and Imaris (Bitplane) software.

High-magnification (63×) time lapses were acquired at 6–8 hpf every 5 s. Data analysis was performed using ImageJ (NIH) software.

To calculate the percentage of ectopic germ cells, PGCs were counted at 24 hpf in the mCherry channel. The average number of ectopic PGCs was counted in percentage to the average total PGC number for the given experiment.

FRET Analysis

The MLC-phosphorylation FRET was performed as previously described [34]. Imaging and analysis for the RhoA- and Rac1-FRET were performed as for the pH index. Imaging for the pH index was performed at 7–9 hpf either on the epifluorescence microscope as described previously [43] or on a LSM710 confocal microscope (40×, numerical aperture [NA] 0.75, pinhole 10 μm, 512 × 512, 7.5 s/frame) controlled by ZEN software (Zeiss). Analysis was done using ImageJ software (for the analysis protocol, see Supplemental Experimental Procedures).

Actin Intensity Measurements

For each mosaic embryo at 8–9 hpf, two time-lapse movies were acquired at 63× magnification; one movie for the PGC containing VasaDsRed signal (PGC with either control morpholino [*COMO*] or *ca15bMO*) and one movie for the PGC without granular labeling ("uninjected," normalization control PGC). Images were processed with ImageJ software (for the analysis protocol, see Supplemental Experimental Procedures).

SUPPLEMENTAL INFORMATION

Supplemental Information includes Supplemental Experimental Procedures, four figures, and four movies and can be found with this article online at http://dx.doi.org/10.1016/j.cub.2015.02.071.

AUTHOR CONTRIBUTIONS

K.T. performed all experimental work except for the experiment described in Figure S4F that was performed by C.G. M.R.-F. generated the *mCherry-F-nos3′UTR* transgenic fish line. K.T., M.R.-F., and E.R. wrote the manuscript and participated in detailed discussions of the study design. E.R. supervised the project.

ACKNOWLEDGMENTS

We thank Dr. B. Mauguis for the ImageJ FRET analysis protocol; I. Halbig, E.-M. Messerschmidt, U. Jordan, I. Sandbote, and P. Knyphausen for excellent technical assistance; Dr. A. Esposito, Prof. M. Knop, and Prof. A. Miyawaki's lab for sharing reagents; and N. Gerigk for the artwork. The work was funded by an ERC advanced grant, the Cells in Motion excellence cluster (CIM), and the German Research Foundation (DFG).

Received: July 10, 2014
Revised: January 6, 2015
Accepted: February 25, 2015
Published: April 2, 2015

REFERENCES

1. Koivusalo, M., Welch, C., Hayashi, H., Scott, C.C., Kim, M., Alexander, T., Touret, N., Hahn, K.M., and Grinstein, S. (2010). Amiloride inhibits macropinocytosis by lowering submembranous pH and preventing Rac1 and Cdc42 signaling. J. Cell Biol. *188*, 547–563.
2. Boedtkjer, E., Praetorius, J., Matchkov, V.V., Stankevicius, E., Mogensen, S., Füchtbauer, A.C., Simonsen, U., Füchtbauer, E.M., and Aalkjaer, C. (2011). Disruption of Na+,HCO_3^- cotransporter NBCn1 (slc4a7) inhibits NO-mediated vasorelaxation, smooth muscle Ca^{2+} sensitivity, and hypertension development in mice. Circulation *124*, 1819–1829.
3. Stock, C., and Schwab, A. (2009). Protons make tumor cells move like clockwork. Pflugers Arch *458*, 981–992.
4. Martin, C., Pedersen, S.F., Schwab, A., and Stock, C. (2011). Intracellular pH gradients in migrating cells. Am. J. Physiol. Cell Physiol. *300*, C490–C495.
5. Schneider, L.A., Korber, A., Grabbe, S., and Dissemond, J. (2007). Influence of pH on wound-healing: a new perspective for wound-therapy? Arch. Dermatol. Res. *298*, 413–420.
6. Sedlakova, O., Svastova, E., Takacova, M., Kopacek, J., Pastorek, J., and Pastorekova, S. (2014). Carbonic anhydrase IX, a hypoxia-induced catalytic component of the pH regulating machinery in tumors. Front. Physiol. *4*, 400.
7. Chiche, J., Ilc, K., Brahimi-Horn, M.C., and Pouysségur, J. (2010). Membrane-bound carbonic anhydrases are key pH regulators controlling tumor growth and cell migration. Adv. Enzyme Regul. *50*, 20–33.
8. Shin, H.J., Rho, S.B., Jung, D.C., Han, I.O., Oh, E.S., and Kim, J.Y. (2011). Carbonic anhydrase IX (CA9) modulates tumor-associated cell migration and invasion. J. Cell Sci. *124*, 1077–1087.
9. Gilmour, K.M., and Perry, S.F. (2009). Carbonic anhydrase and acid-base regulation in fish. J. Exp. Biol. *212*, 1647–1661.
10. Casey, J.R., Grinstein, S., and Orlowski, J. (2010). Sensors and regulators of intracellular pH. Nat. Rev. Mol. Cell Biol. *11*, 50–61.
11. Vaughan-Jones, R.D., Spitzer, K.W., and Swietach, P. (2009). Intracellular pH regulation in heart. J. Mol. Cell. Cardiol. *46*, 318–331.
12. Hayashi, H., Aharonovitz, O., Alexander, R.T., Touret, N., Furuya, W., Orlowski, J., and Grinstein, S. (2008). Na+/H+ exchange and pH regulation in the control of neutrophil chemokinesis and chemotaxis. Am. J. Physiol. Cell Physiol. *294*, C526–C534.
13. Friedl, P., and Wolf, K. (2003). Tumour-cell invasion and migration: diversity and escape mechanisms. Nat. Rev. Cancer *3*, 362–374.
14. Cojoc, M., Peitzsch, C., Trautmann, F., Polishchuk, L., Telegeev, G.D., and Dubrovska, A. (2013). Emerging targets in cancer management: role of the CXCL12/CXCR4 axis. Onco Targets Ther. *6*, 1347–1361.
15. Mitchell, B., and Mahalingam, M. (2014). The CXCR4/CXCL12 axis in cutaneous malignancies with an emphasis on melanoma. Histol. Histopathol. *29*, 1539–1546.
16. Polyak, K., and Weinberg, R.A. (2009). Transitions between epithelial and mesenchymal states: acquisition of malignant and stem cell traits. Nat. Rev. Cancer *9*, 265–273.
17. Sahai, E. (2005). Mechanisms of cancer cell invasion. Curr. Opin. Genet. Dev. *15*, 87–96.
18. Tarbashevich, K., and Raz, E. (2010). The nuts and bolts of germ-cell migration. Curr. Opin. Cell Biol. *22*, 715–721.
19. Shimozono, S., Hosoi, H., Mizuno, H., Fukano, T., Tahara, T., and Miyawaki, A. (2006). Concatenation of cyan and yellow fluorescent proteins for efficient resonance energy transfer. Biochemistry *45*, 6267–6271.
20. Esposito, A., Gralle, M., Dani, M.A., Lange, D., and Wouters, F.S. (2008). pHlameleons: a family of FRET-based protein sensors for quantitative pH imaging. Biochemistry *47*, 13115–13126.
21. Köprunner, M., Thisse, C., Thisse, B., and Raz, E. (2001). A zebrafish nanos-related gene is essential for the development of primordial germ cells. Genes Dev. *15*, 2877–2885.
22. Reichman-Fried, M., Minina, S., and Raz, E. (2004). Autonomous modes of behavior in primordial germ cell migration. Dev. Cell *6*, 589–596.
23. Kneen, M., Farinas, J., Li, Y., and Verkman, A.S. (1998). Green fluorescent protein as a noninvasive intracellular pH indicator. Biophys. J. *74*, 1591–1599.

24. Kumar, K. (2014). pH sensor using superfolder green fluorescent protein for intracellular studies. MS thesis. (Tampere: Tampere University of Technology).
25. Swietach, P., Wigfield, S., Cobden, P., Supuran, C.T., Harris, A.L., and Vaughan-Jones, R.D. (2008). Tumor-associated carbonic anhydrase 9 spatially coordinates intracellular pH in three-dimensional multicellular growths. J. Biol. Chem. *283*, 20473–20483.
26. Hartwig, J., Tarbashevich, K., Seggewiß, J., Stehling, M., Bandemer, J., Grimaldi, C., Paksa, A., Groß-Thebing, T., Meyen, D., and Raz, E. (2014). Temporal control over the initiation of cell motility by a regulator of G-protein signaling. Proc. Natl. Acad. Sci. USA *111*, 11389–11394.
27. Wang, C., and Lehmann, R. (1991). Nanos is the localized posterior determinant in Drosophila. Cell *66*, 637–647.
28. Subramaniam, K., and Seydoux, G. (1999). nos-1 and nos-2, two genes related to Drosophila nanos, regulate primordial germ cell development and survival in Caenorhabditis elegans. Development *126*, 4861–4871.
29. Mosquera, L., Forristall, C., Zhou, Y., and King, M.L. (1993). A mRNA localized to the vegetal cortex of Xenopus oocytes encodes a protein with a nanos-like zinc finger domain. Development *117*, 377–386.
30. Wang, H., Teng, Y., Xie, Y., Wang, B., Leng, Y., Shu, H., and Deng, F. (2013). Characterization of the carbonic anhydrases 15b expressed in PGCs during early zebrafish development. Theriogenology *79*, 443–452.
31. Hilvo, M., Tolvanen, M., Clark, A., Shen, B., Shah, G.N., Waheed, A., Halmi, P., Hänninen, M., Hämäläinen, J.M., Vihinen, M., et al. (2005). Characterization of CA XV, a new GPI-anchored form of carbonic anhydrase. Biochem. J. *392*, 83–92.
32. Doitsidou, M., Reichman-Fried, M., Stebler, J., Köprunner, M., Dörries, J., Meyer, D., Esguerra, C.V., Leung, T., and Raz, E. (2002). Guidance of primordial germ cell migration by the chemokine SDF-1. Cell *111*, 647–659.
33. Dumstrei, K., Mennecke, R., and Raz, E. (2004). Signaling pathways controlling primordial germ cell migration in zebrafish. J. Cell Sci. *117*, 4787–4795.
34. Blaser, H., Reichman-Fried, M., Castanon, I., Dumstrei, K., Marlow, F.L., Kawakami, K., Solnica-Krezel, L., Heisenberg, C.P., and Raz, E. (2006). Migration of zebrafish primordial germ cells: a role for myosin contraction and cytoplasmic flow. Dev. Cell *11*, 613–627.
35. Pandey, K., Dhoke, R.R., Rathore, Y.S., Nath, S.K., Verma, N., Bawa, S., and Ashish, F. (2014). Low pH overrides the need of calcium ions for the shape-function relationship of calmodulin: resolving prevailing debates. J. Phys. Chem. B *118*, 5059–5074.
36. Matsumura, F. (2005). Regulation of myosin II during cytokinesis in higher eukaryotes. Trends Cell Biol. *15*, 371–377.
37. Moussavi, R.S., Kelley, C.A., and Adelstein, R.S. (1993). Phosphorylation of vertebrate nonmuscle and smooth muscle myosin heavy chains and light chains. Mol. Cell. Biochem. *127-128*, 219–227.
38. Paradiso, A., Cardone, R.A., Bellizzi, A., Bagorda, A., Guerra, L., Tommasino, M., Casavola, V., and Reshkin, S.J. (2004). The Na+-H+ exchanger-1 induces cytoskeletal changes involving reciprocal RhoA and Rac1 signaling, resulting in motility and invasion in MDA-MB-435 cells. Breast Cancer Res. *6*, R616–R628.
39. Kardash, E., Reichman-Fried, M., Maitre, J.L., Boldajipour, B., Papusheva, E., Messerschmidt, E.M., Heisenberg, C.P., and Raz, E. (2010). A role for Rho GTPases and cell-cell adhesion in single-cell motility in vivo. Nat. Cell Biol. *12*, 47–53.
40. Hawkins, M., Pope, B., Maciver, S.K., and Weeds, A.G. (1993). Human actin depolymerizing factor mediates a pH-sensitive destruction of actin filaments. Biochemistry *32*, 9985–9993.
41. Reshkin, S.J., Cardone, R.A., and Harguindey, S. (2013). Na+-H+ exchanger, pH regulation and cancer. Recent Pat. Anticancer Drug Discov. *8*, 85–99.
42. Amith, S.R., and Fliegel, L. (2013). Regulation of the Na+/H+ Exchanger (NHE1) in Breast Cancer Metastasis. Cancer Res. *73*, 1259–1264.
43. Kardash, E., Bandemer, J., and Raz, E. (2011). Imaging protein activity in live embryos using fluorescence resonance energy transfer biosensors. Nat. Protoc. *6*, 1835–1846.